Silicene catalyst for CO_2 hydrogenation: the number of layers controls selectivity

Si Zhou,[a,b] Wei Pei,[a] Jijun Zhao*[a,c] and Aijun Du*[b]

[a]*Key Laboratory of Materials Modification by Laser, Ion and Electron Beams, Ministry of Education, Dalian University of Technology, Dalian 116024, China*

[b]*School of Chemistry, Physics and Mechanical Engineering, Science and Engineering Faculty, Queensland University of Technology, Gardens Point Campus, Brisbane, QLD 4001, Australia*

[c]*Beijing Computational Science Research Center, Beijing 100094, China*

* Corresponding authors. Email: zhaojj@dlut.edu.cn (J. Zhao), aijun.du@qut.edu.au (A. Du)

Table S1 Test calculations on adsorption energies of a CO_2 molecule on the supported monolayer silicene with the Si(√7 × √7)/Ag(√13 × √13) superstructure, and on the (111) surface of bulk silicon. For the silicene superstructure, the Ag substrate is represented by a slab mode with 3, 4, 5 and 6 layers of Ag atoms, respectively. The bulk silicon is mimicked by a slab model with 3, 4, 5 and 6 layers of Si atoms, respectively, with the (111) surface exposed and the bottom layer Si atoms terminated by H atoms. According to the CO_2 adsorption energies shown below, a 3-layer slab is fairly good enough to model Ag substrate, while the adsorption energy well reaches convergence by using a 5-layer slab for bulk silicon

Number of substrate layers	Si√7/Ag√13 superstructure	Number of Si layers	Bulk Si(111) surface
3	−0.49 eV	3	−1.40 eV
4	−0.47 eV	4	−1.36 eV
5	−0.48 eV	5	−1.35 eV
6	−0.47 eV	6	−1.35 eV

Table S2 Zero-point energy (ZPE) and entropic correction (*TS*) at T = 298 K for the molecules and intermediate species involved in CO_2 hydrogenation reaction, obtained by calculating their vibrational frequencies by VASP.[1] The entropy values of molecules are taken from the NIST-JANAF thermodynamics table.[2] The (ZPE – *TS*) values of reaction intermediates adsorbed on bilayer silicene on Ag(111) substrate are presented and used throughout our calculations, which are close to the values for the monolayer and other few-layer systems

Species	ZPE (eV)	*TS* (eV)	ZPE−*TS* (eV)
H_2	0.29	0.41	−0.12
H_2O	0.60	0.59	0.01
CO	0.14	0.62	−0.48
CO_2	0.31	0.67	−0.35
CH_2O	0.72	0.68	0.04
HCOOH	0.92	1.02	−0.10
CH_3OH	1.39	0.79	0.60
CH_4	1.20	0.58	0.61
CO_2*	0.32	0.13	0.19
HCOO*	0.60	0.21	0.39
COOH*	0.58	0.13	0.45
CO*	0.21	0.12	0.09
HCOOH*	0.94	0.15	0.79
HCO*	0.47	0.16	0.31
HCOH*	0.79	0.14	0.65
H_2COH*	1.10	0.16	0.94
CH_2*	0.67	0.06	0.61
CH_3*	0.97	0.13	0.84

Table S3 Geometrical, adsorption and electronic properties of monolayer silicene on Ag(111) substrate in the Si(√7 × √7)/Ag(√13 × √13), Si(√7 × √7)/Ag(2√3 × 2√3) and Si(3 × 3)/Ag(4 × 4) phases, including average distance (*d*) between silicene and Ag substrate and corresponding charge transfer to each Si atom (CT), adsorption energy and kinetic barrier for CO_2 chemisorption (E_a^{CO2}), and lower bound and center of energies of surface dangling bond states (E_0, ε_{DB}).

system	*d* (Å)	CT (*e*)	ΔE_{CO2} (eV)	E_a^{CO2} (eV)	E_0 (eV)	ε_{DB} (eV)
Si√7/Ag√13	2.44	0.04	–0.49	0.38	–3.0	–1.17
Si√7/Ag2√3	2.51	0.04	–0.46	0.40	–3.0	–1.20
Si3/Ag4	2.50	0.04	–0.40	0.42	–3.4	–1.25

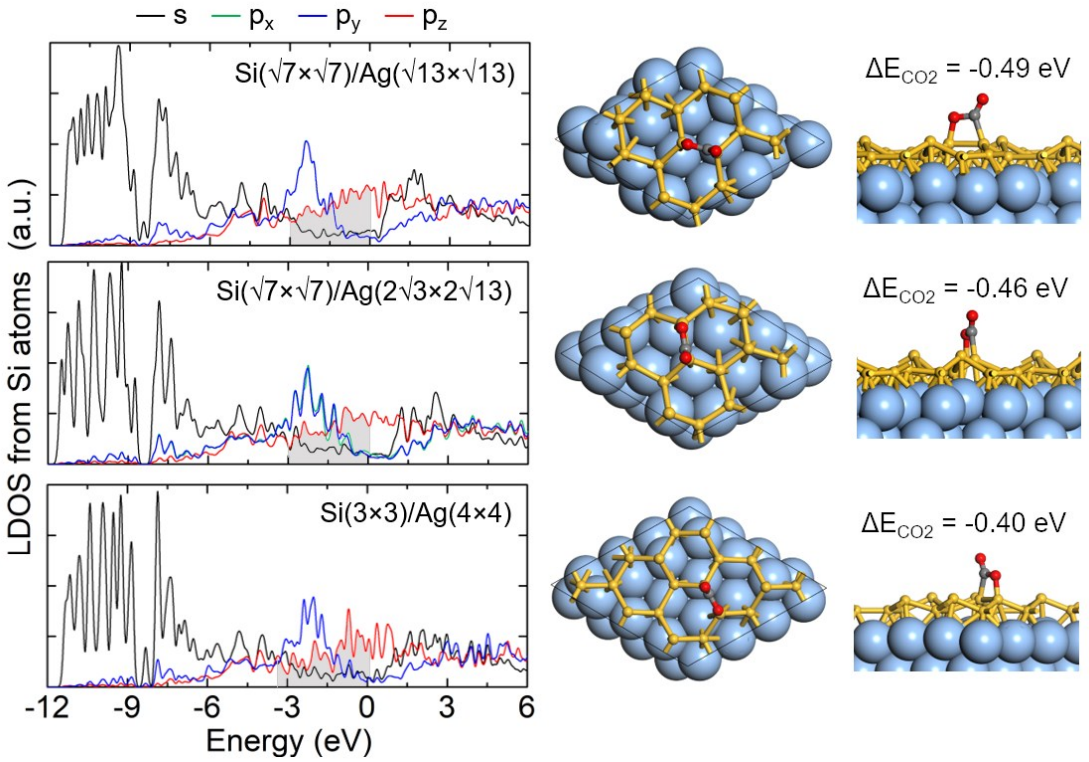

Fig. S1 Left panels: local density of states (LDOS) from Si atoms in monolayer silicene/Ag superstructures projected onto various atomic orbitals. The surface dangling bond states are shadowed. The Fermi level is set to zero. Right panels: top and side views of structures of silicene/Ag superstructures with adsorption of a CO_2 molecule. The Si and Ag atoms are shown in yellow and blue colors, respectively. The CO_2 adsorption energies (ΔE_{CO2}) are indicated for each system.

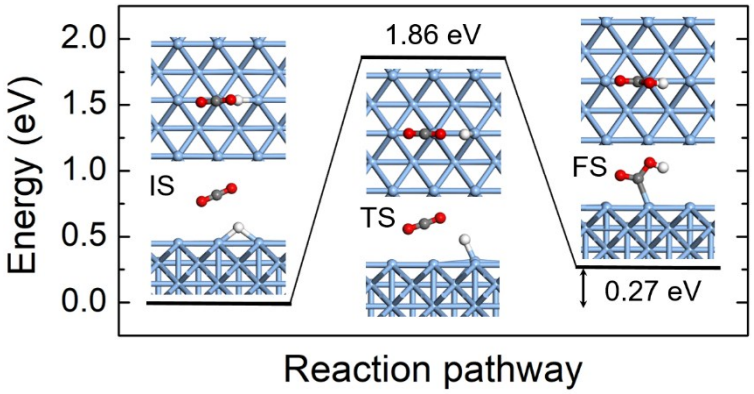

Fig. S2 Reaction of CO_2 with a H adatom to form COOH* species adsorbed on the Ag(110) surface. The energies and atomic structures are presented for the initial state (IS), transition state (TS) and final state (FS). The H, C, O and Ag atoms are shown in white, grey, red and blue colors, respectively. The supercell consists of 3 × 4 unit cells of Ag(110) surface for the lateral dimension and six atomic layers with vacuum region of 16 Å for the vertical direction.

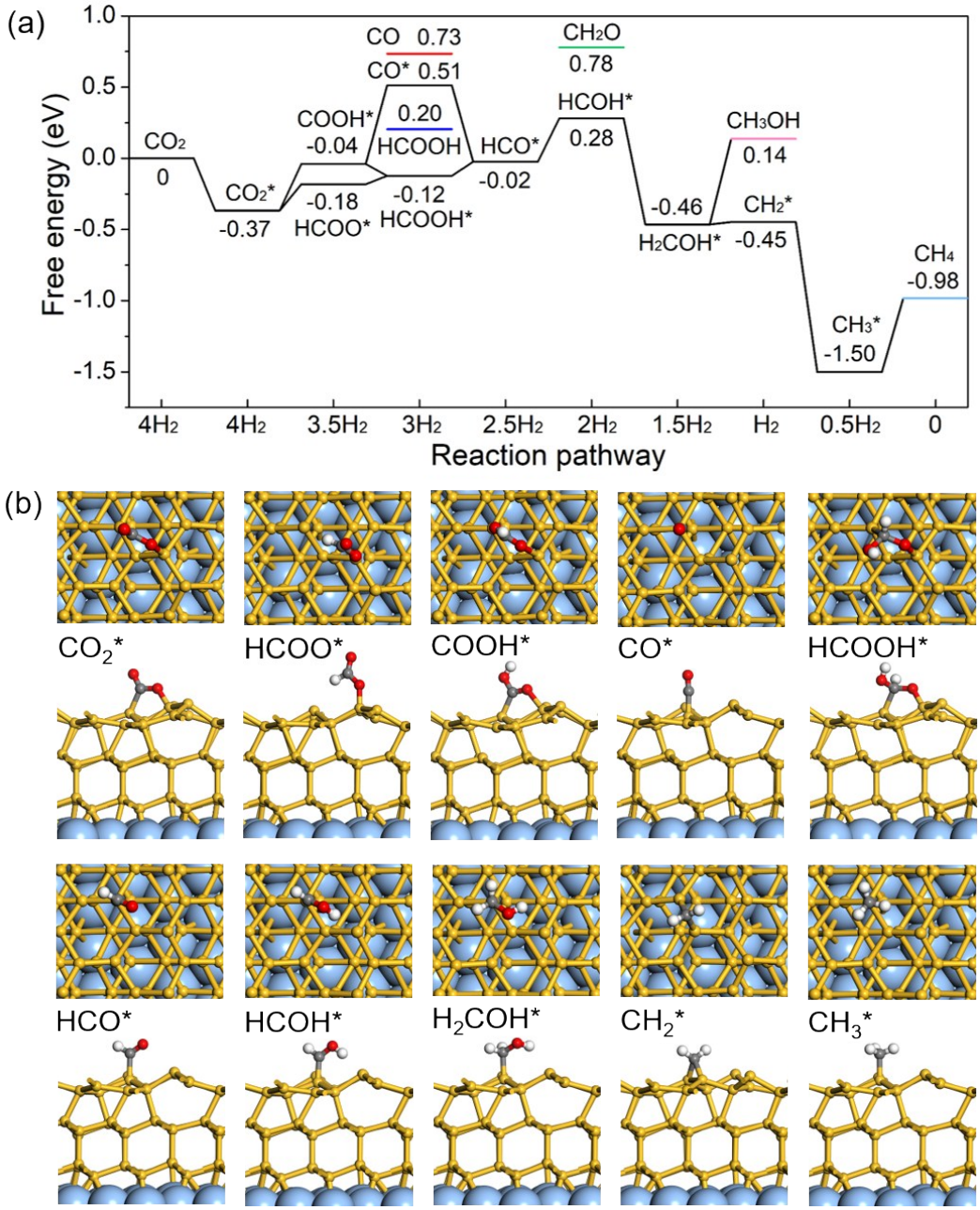

Fig. S3 (a) Free energy diagram of CO_2 hydrogenation on trilayer silicene on Ag(111). The colored line segments show the formation of various products. The asterisk (*) indicates chemisorption of reaction intermediates on the catalyst surface. The relative free energy (in eV) is given for each elemental step. (b) Atomic structures of reaction intermediates of CO_2 hydrogenation on trilayer silicene on Ag(111). The H, C, O, Si and Ag atoms are shown in white, grey, red, yellow and blue colors, respectively.

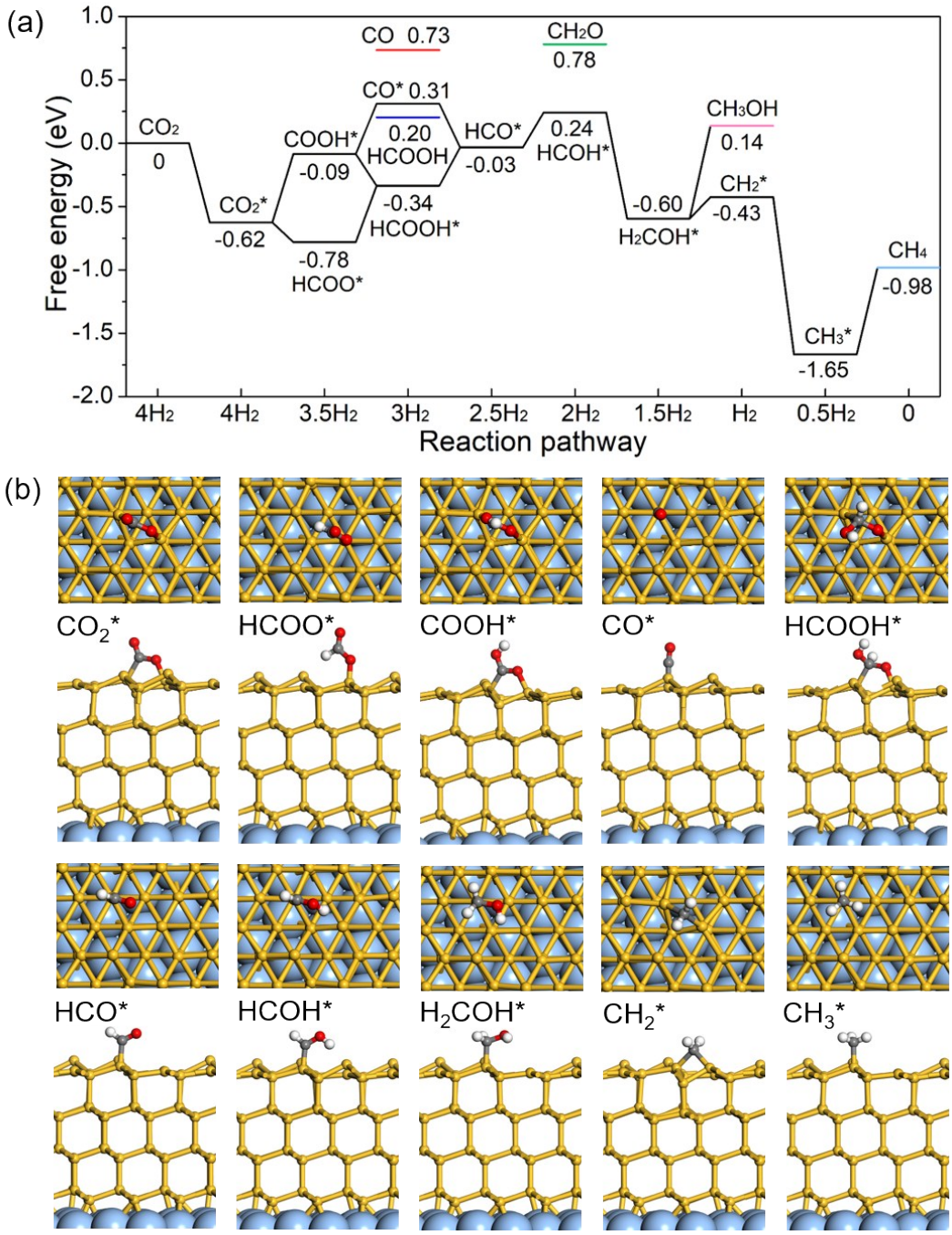

Fig. S4 (a) Free energy diagram of CO_2 hydrogenation on tetralayer silicene on Ag(111). The colored line segments show the formation of various products. The asterisk (*) indicates chemisorption of reaction intermediates on the catalyst surface. The relative free energy (in eV) is given for each elemental step. (b) Atomic structures of reaction intermediates of CO_2 hydrogenation on tetralayer silicene on Ag(111). The H, C, O, Si and Ag atoms are shown in white, grey, red, yellow and blue colors, respectively.

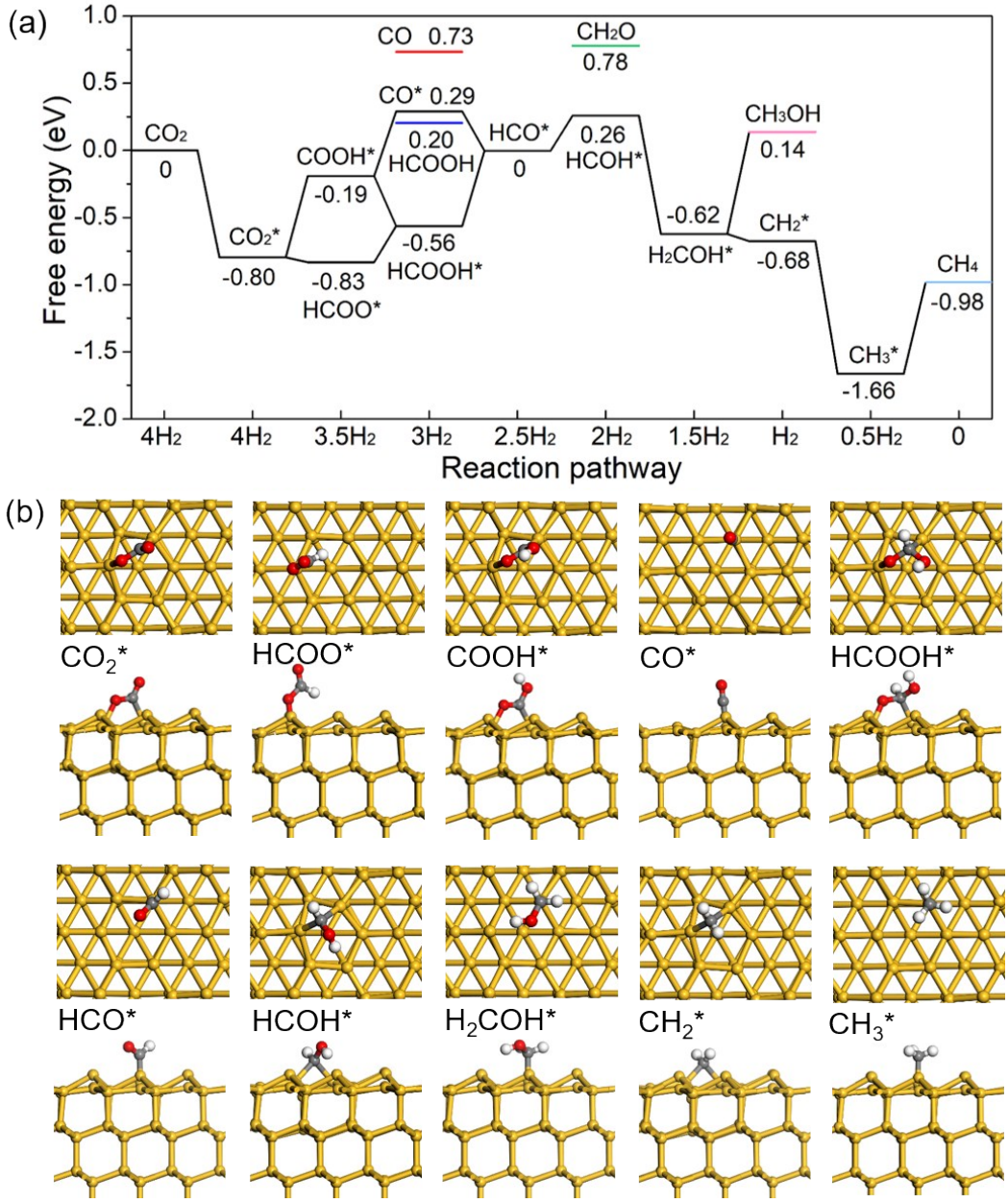

Fig. S5 (a) Free energy diagram of CO_2 hydrogenation on bulk Si(111) surface. The colored line segments show the formation of various products. The asterisk (*) indicates chemisorption of reaction intermediates on the catalyst surface. The relative free energy (in eV) is given for each elemental step. (b) Atomic structures of reaction intermediates of CO_2 hydrogenation on bulk Si(111) surface. The H, C, O and Si atoms are shown in white, grey, red and yellow colors, respectively.

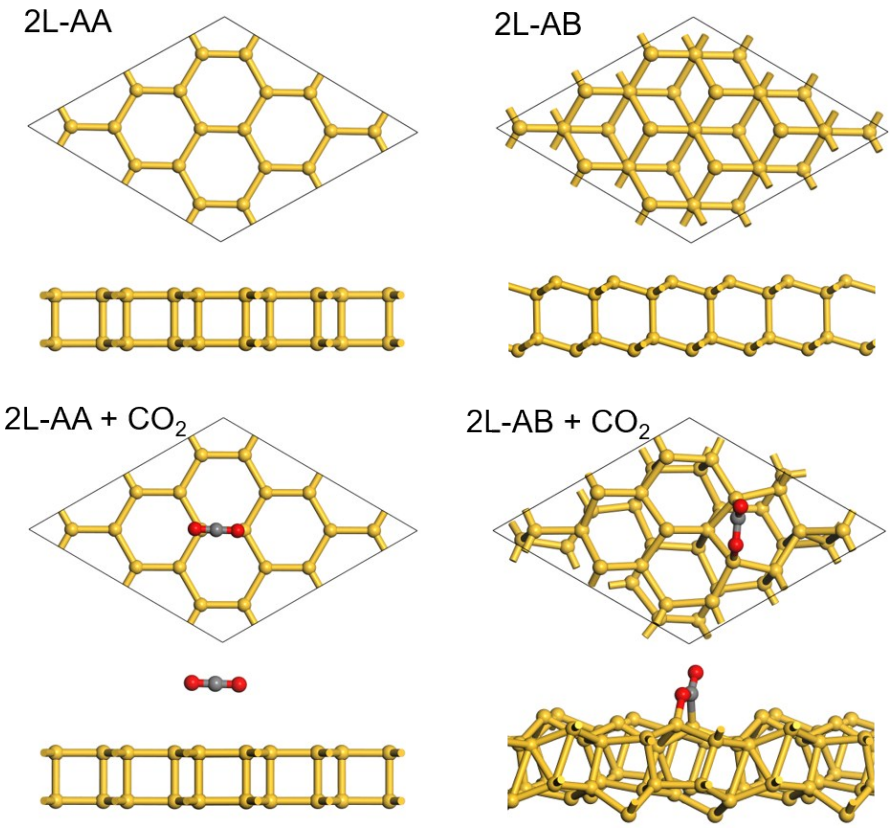

Fig. S6 Atomic structures of freestanding bilayer silicene in AA (2L-AA) and AB (2L-AB) stacking before and after adsorption of a CO_2 molecule (top panel: top view; bottom panel: side view). The black box indicates the lateral dimension of the supercell consisting of 3×3 silicene unit cells. The C, O and Si atoms are shown in grey, red and yellow colors, respectively. Bilayer silicene with AA and AB stacking are very close in energy, with the former lower by 0.025 eV per Si atom than the latter. The system with AA stacking geometry has a flat surface and is inert to CO_2. In contrast, the structure of bilayer silicene with AB stacking is severely destructed and becomes disordered upon CO_2 adsorption.

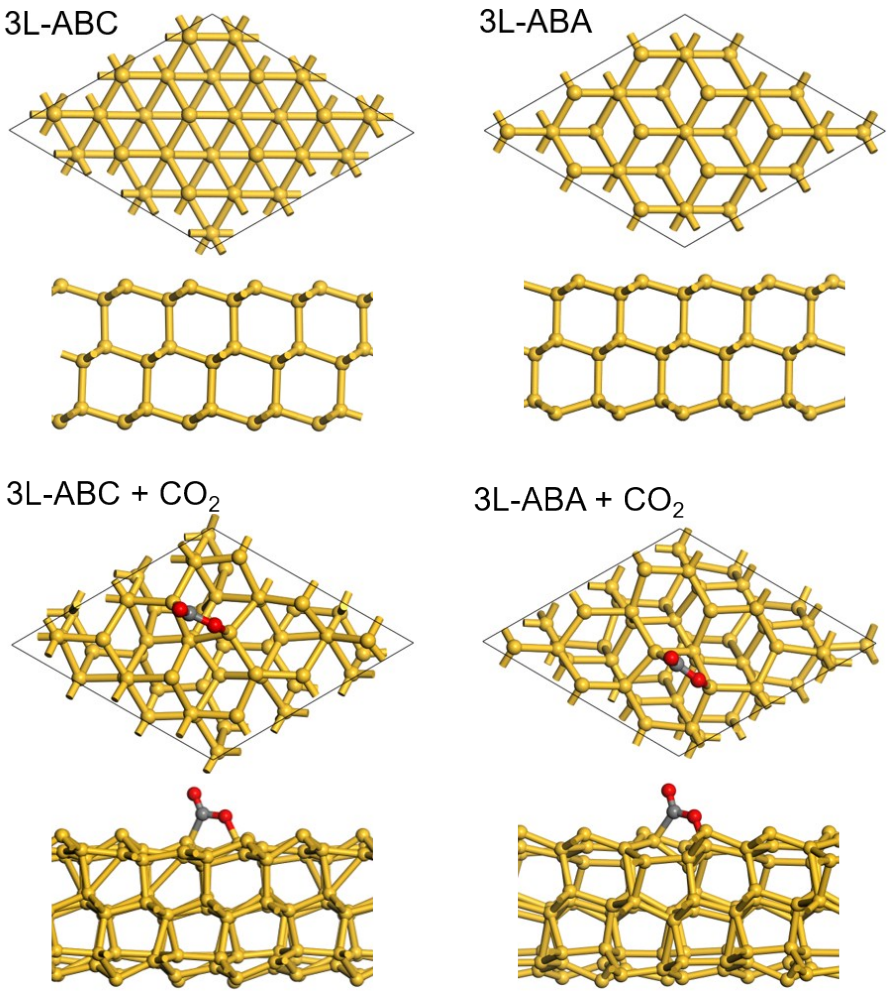

Fig. S7 Atomic structures of freestanding trilayer silicene in ABC (3L-ABC) and ABA (3L-ABA) stacking before and after adsorption of a CO_2 molecule (top panel: top view; bottom panel: side view). The black box indicates the lateral dimension of the supercell consisting of 3×3 silicene unit cells. The C, O and Si atoms are shown in grey, red and yellow colors, respectively. Trilayer silicene with ABC and ABA stacking are very close in energy, with the former lower by 0.017 eV per Si atom than the latter. For both systems, adsorption of CO_2 induces severe structural distortion and reconstruction.

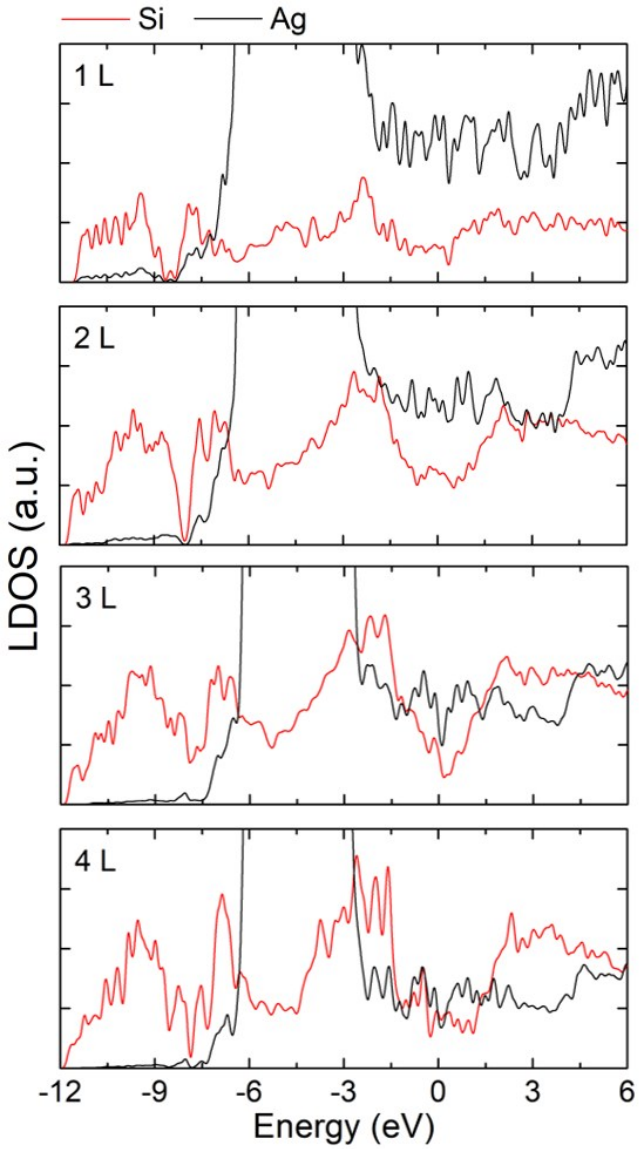

Fig. S8 Local density of states (LDOS) of Si and Ag atoms from monolayer and few-layer silicene on Ag(111) substrate. Color scheme: red for Si and black for Ag. The Fermi level is set to zero.

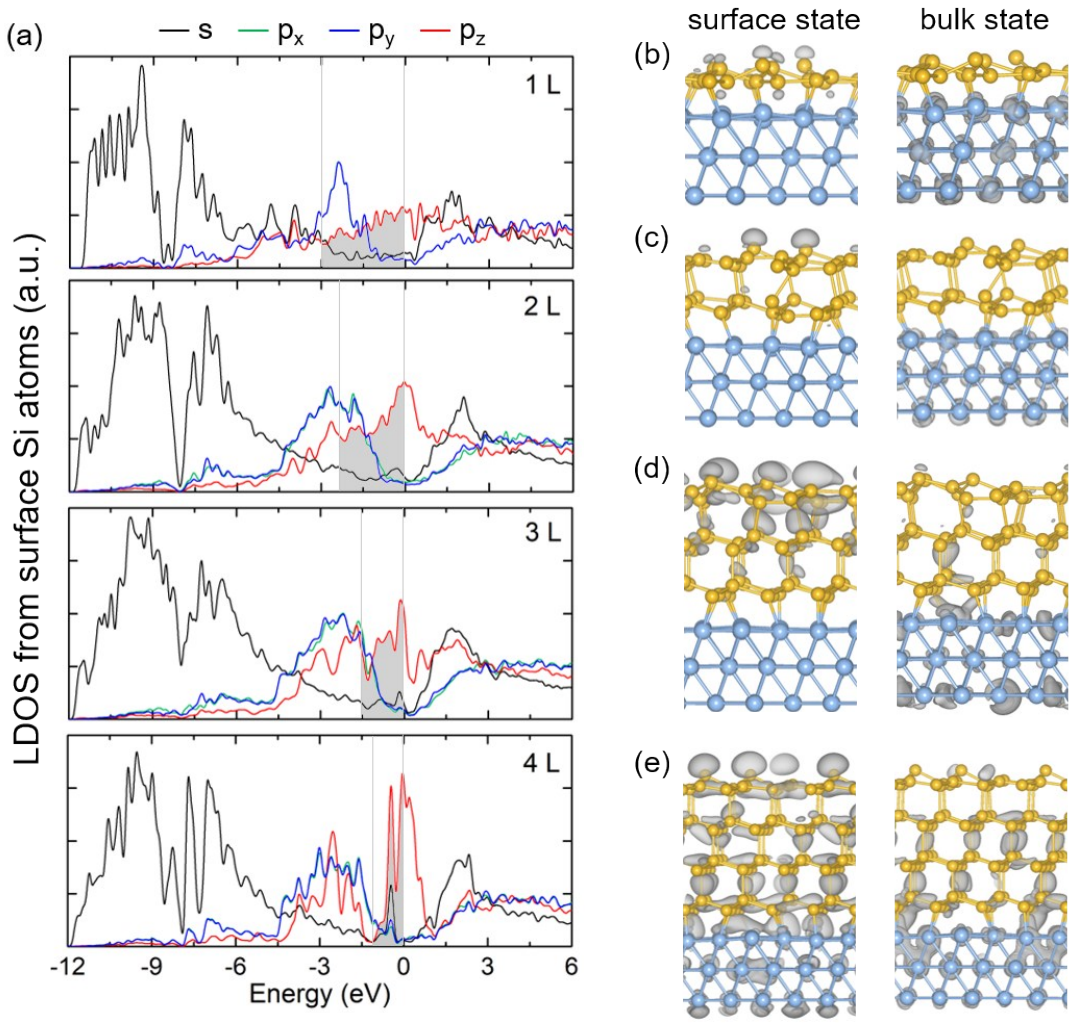

Fig. S9 (a) Local density of states (LDOS) from surface Si atoms in monolayer and few-layer silicene on Ag(111) projected onto various atomic orbitals. The Fermi level is set to zero. The surface dangling bond states are shadowed. The lower bound of these surface states is determined by examining the partial charge densities at different energies. The (occupied) surface states are located at relatively higher energy levels close to the Fermi energy, and their partial charge densities (grey colors) distribute mainly on the top layer silicene, as shown in the left panels of (b-e). For the electronic states at deeper energy levels, the partial charge densities start to spread to the bottom layer silicene and Ag substrate, which are identified as bulk states and shown in the right panels of (b-e). An isosurface value of 5×10^{-4} e/Å^3 was used for charge densities in (b-e).

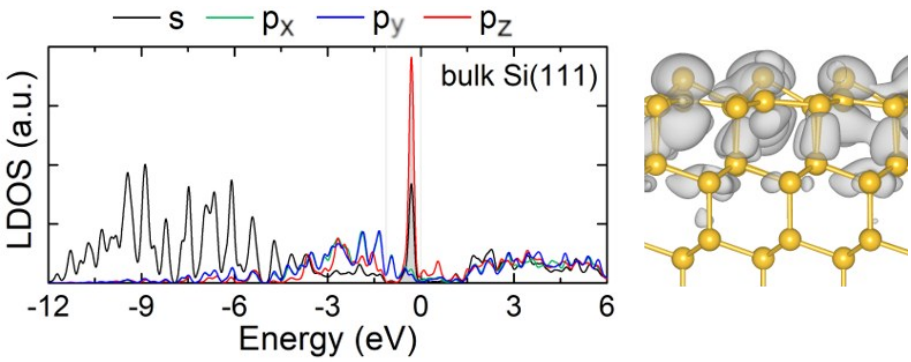

Fig. S10 Local density of states (LDOS) of surface Si atoms from bulk Si(111) projected onto various atomic orbitals. The surface dangling bond states are shadowed. The Fermi level is set to zero. Partial charge density distributions (grey colors) of the surface dangling bonds at Fermi level is shown on the right panel, with an isosurface value of 5×10^{-4} e/Å^3.

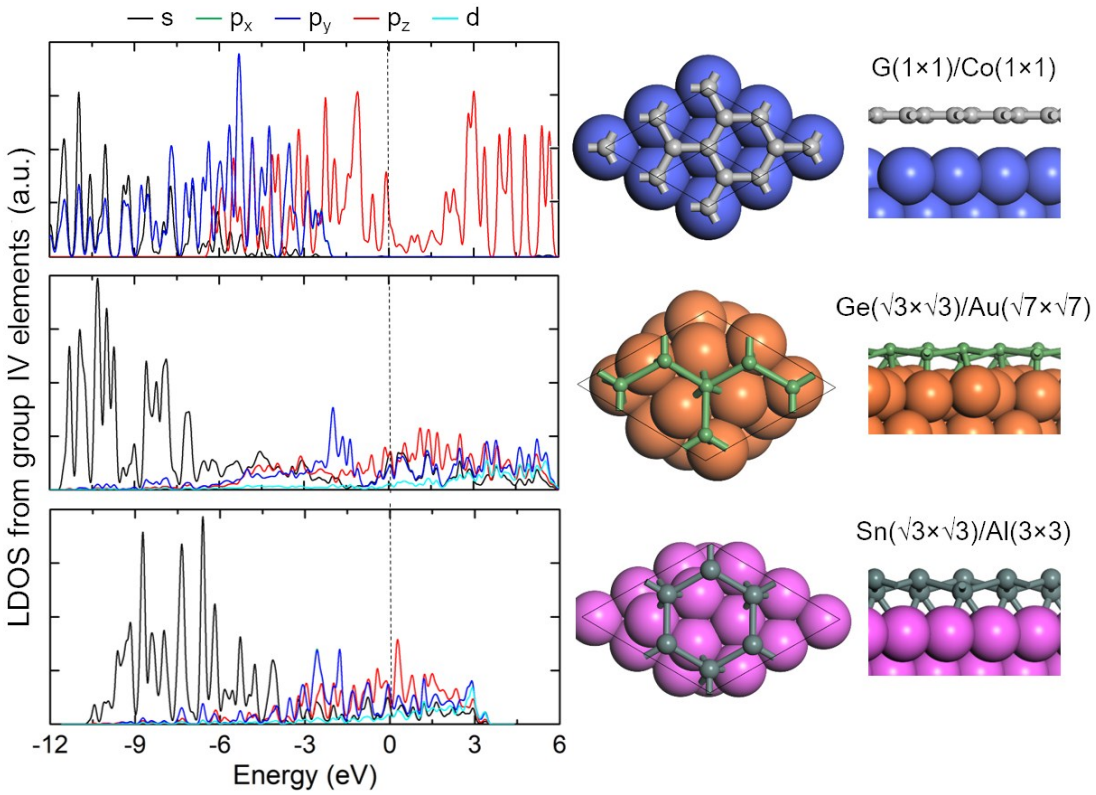

Fig. S11 Left panels: local density of states (LDOS) from C, Ge or Sn atoms in monolayer graphene on Co(111), germanene on Au(111) and stanene on Al(111) substrates projected onto various atomic orbitals. The Fermi level is set to zero. Right panels: top and side views of the corresponding superstructures of graphene(1 × 1)/Co(1 × 1), germanene(√3 × √3)/Au(√7 × √7) and stanene(√3 × √3)/Al(3 × 3).[3-5] To explore the adsorption of CO_2 on these 2D materials, 5 × 5, 2 × 2 and 2 × 2 superstructures were adopted for the substrate-supported graphene, germanene and stanene systems, respectively, with lateral dimension of supercells of 12.5 ~ 17.2 Å. Our calculations show that none of them can chemisorb CO_2 molecule. The supported graphene has weak van der Waals interaction with Co substrate, with interlayer distance of 2.92 Å. It remains flat surface with π conjugation little intact. Monolayer germanene and stanene on metal substrates have buckled structures as that of silicene. However, they show less surface dangling states near the Fermi level compared to the LDOS of silicene/Ag superstructure in Figure S9a, which may be ascribed to the stronger metallicity of germanene and stanene than silicene.

References

1 K. Reuter and M. Scheffler, *Phys. Rev. B*, 2001, **65**, 035406.

2 M. W. Chase, *NIST-JANAF Thermochemical Tables, 4th ed.*, American Chemical Society and American Institute of Physics Press, New York, 1998.

3 D. Prezzi, D. Eom, K. T. Rim, H. Zhou, S. Xiao, C. Nuckolls, T. F. Heinz, G. W. Flynn, M. S. Hybertsen, *ACS Nano*, 2014, **8**, 5765-5773.

4 M. E. Dávila and G. Le Lay, *Sci. Rep.*, 2016, **6**, 20714.

5 N. Gao, H. Liu, S. Zhou, Y. Bai and J. Zhao, *J. Phys. Chem. C*, 2017, **121**, 5123-5129.